

Chapter IV

Fitting results for the solar flares of 1981 July 20, 1982 January 2, and 1978 September 23

The Flare of 1981 July 20

Fitting result of this flare in each energy is in the table 4.1. The Energies vary from E1 to E45 (added E4 and E5) and λ vary from 0.05 AU to 0.25 AU. The suitable λ for E1 is 0.08 AU (least Chi-square in column 2). For E2, E3, and E45 the suitable λ is 0.10, 0.12, and 0.12 respectively. The continuous line in the graph is the calculated result and the circles with error bars are the measured data. Graphs of the fitting is in the figures 4.1, 4.3, 4.5, and 4.7 respectively. Graphs in the figure 4.2, 4.4, 4.6, and 4.8 show the anisotropy \times intensity vs. time. If we compare the graphs of anisotropy with intensity, they are different for the two types of data. So, this is the reason why we determine the flare of 1981 July 20 only in the intensity. The injection profile of the best λ in each energy is shown in the figure 4.9 for E1, 4.10 for E2, 4.11 for E3, and 4.12 for E45.

The fitting of the intensity without energy separation resulted in the Table 4.2. The λ values are from 0.08 AU to 0.45 AU and the Chi-square is 39.335 the least in the table. The fitting of the intensity when not separating energies is best for $\lambda=0.10$ AU, about the average of the fitting results of determining energies. A graph of this fitting is shown in figure 4.13 and graph of the injection profile is shown in figure 4.14.

The Flare of 1982 January 2

Fitting result of this flare in intensity is in the table 4.3. The λ is vary from 0.15 AU to 0.45 AU. The best λ of this flare is 0.20 AU at the least chi-

λ	E1	E2	E3	E45
0.05	24.793952	3.985746	3.609900	14.334657
0.08	2.427836	1.282712	1.413924	1.472458
0.10	3.747616	1.112697	1.201160	1.108753
0.12	7.971596	1.562227	1.182007	0.994798
0.15	14.320825	2.338675	1.293701	1.006499
0.20	29.741747	3.251940	1.434680	1.004674
0.25	48.725109	9.674932	2.906644	1.684526

Table 4.1: Chi-square values for the gradual flare of 1981 July 20 in each energy.

λ	Chi-square
0.08	177.273064
0.10	39.335159
0.12	66.501164
0.15	324.048913
0.20	1083.483626
0.25	2072.158643
0.45	6770.513462

Table 4.2: Chi-square values for the gradual flare of 1981 July 20.

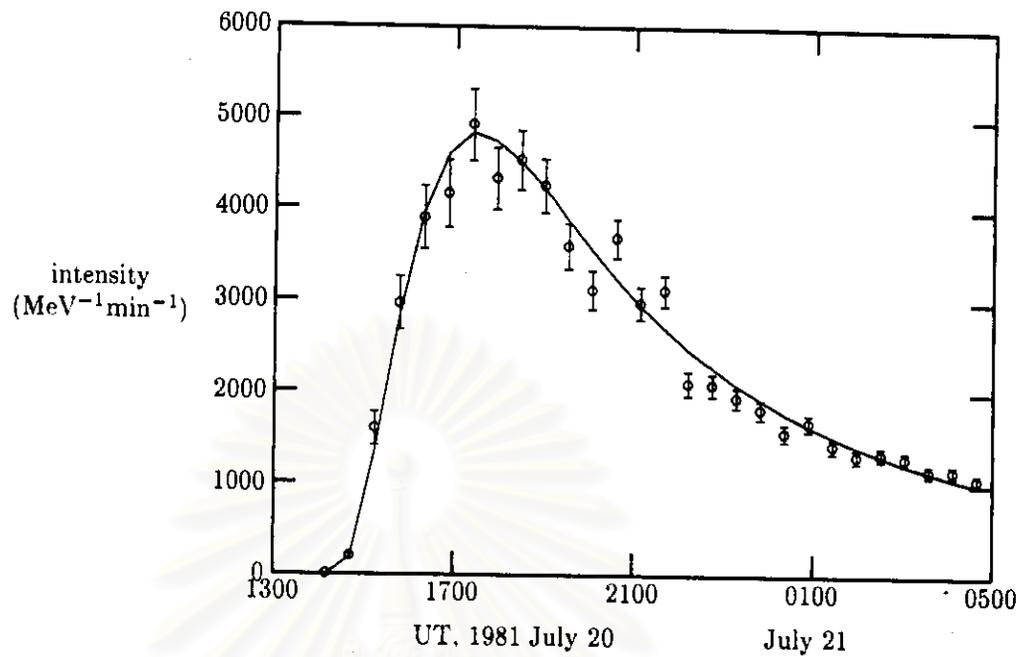


Figure 4.1: Graph of data and simulation of intensity $\lambda=0.08$ AU for energy 1 Flare July 20,81.

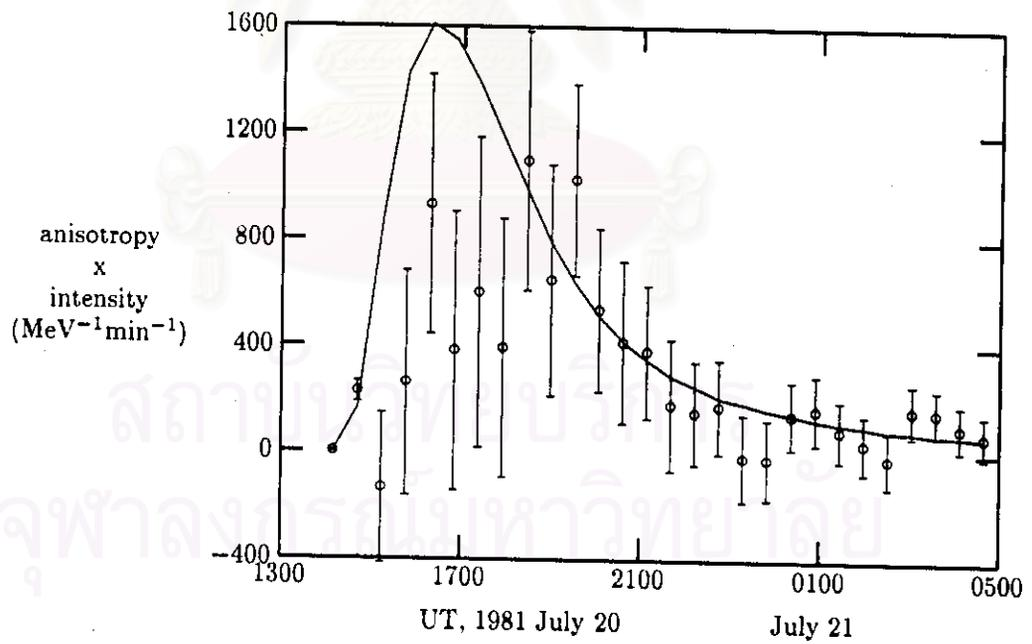


Figure 4.2: Graph of data and simulation of anisotropy $\lambda=0.08$ AU for energy 1 Flare July 20,81. The anisotropy is poorly fit because of rapid manetic field fluctuations.

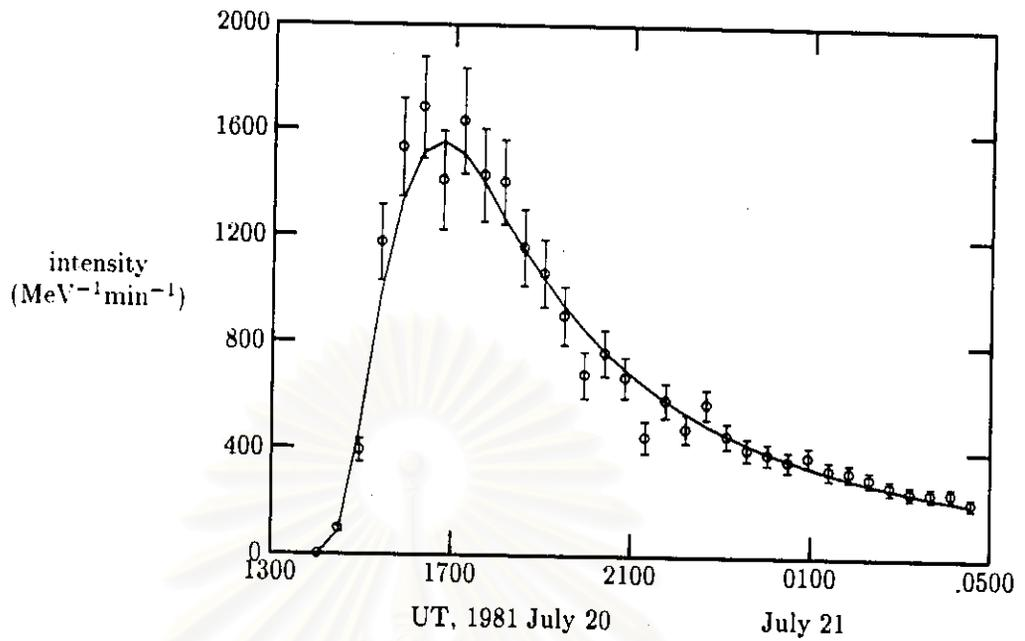


Figure 4.3: Graph of data and simulation of intensity $\lambda=0.10$ AU for energy 2 Flare July 20.81.

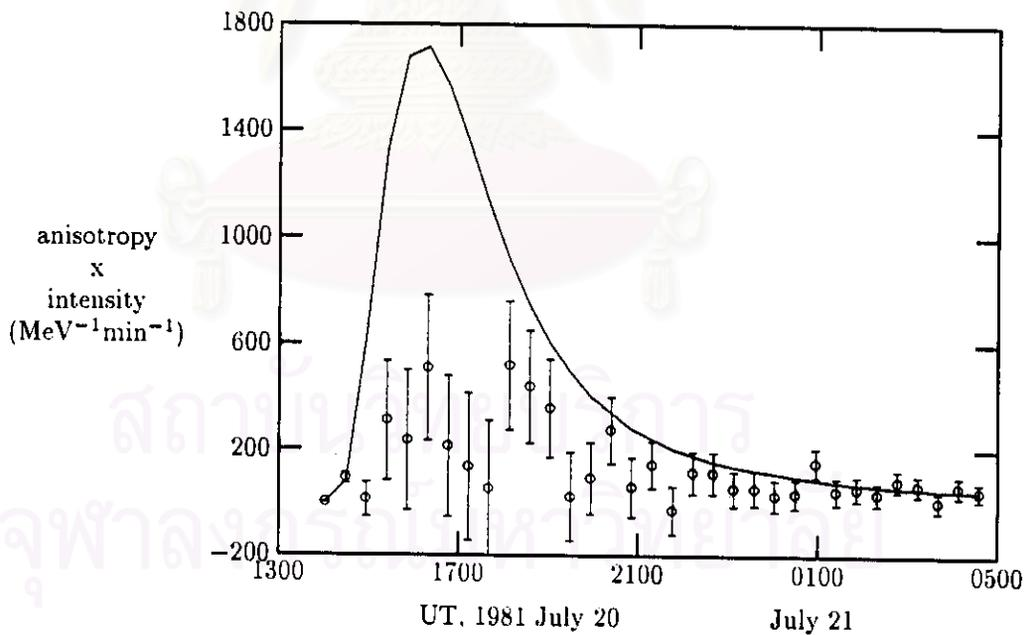


Figure 4.4: Graph of data and simulation of anisotropy $\lambda=0.10$ AU for energy 2 Flare July 20.81. The anisotropy is poorly fit because of rapid magnetic field fluctuations.

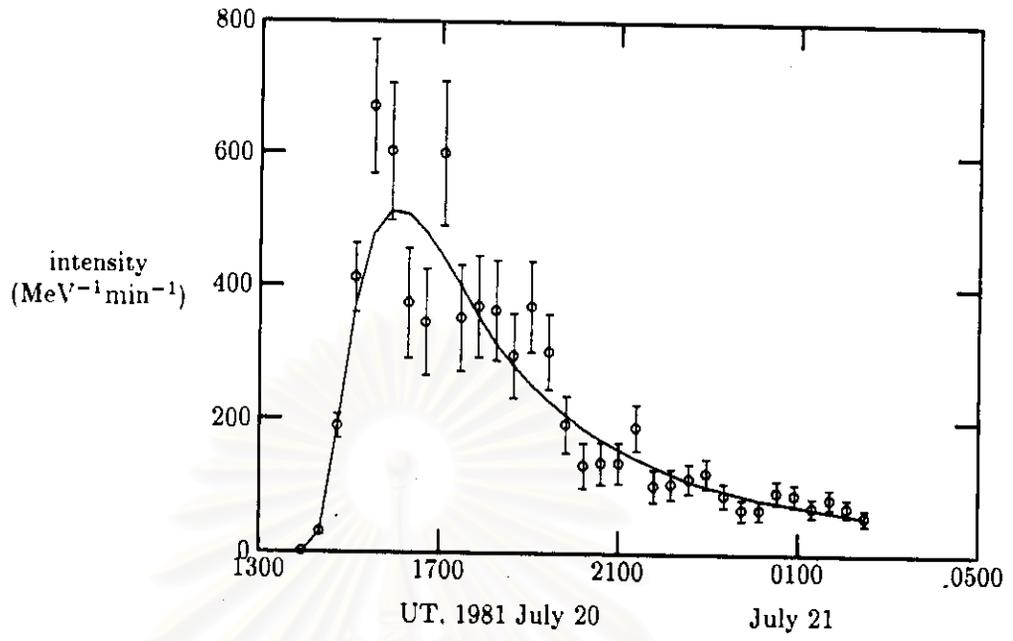


Figure 4.5: Graph of data and simulation of intensity $\lambda=0.12$ AU for energy 3 Flare July 20,81.

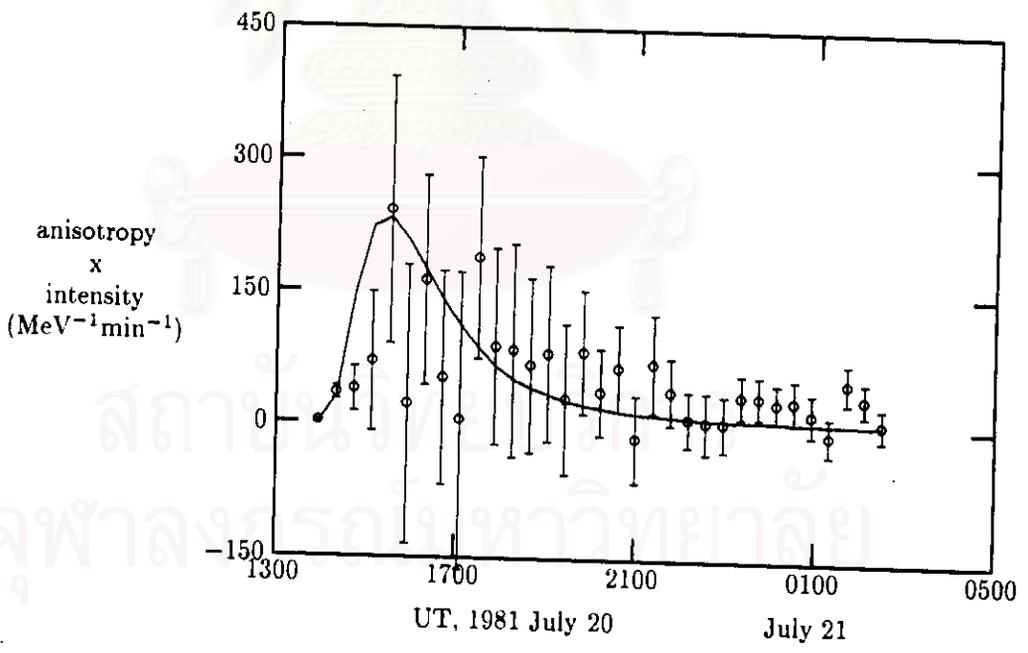


Figure 4.6: Graph of data and simulation of anisotropy $\lambda=0.12$ AU for energy 3 Flare July 20,81. The anisotropy is poorly fit because of rapid manetic field fluctuations.

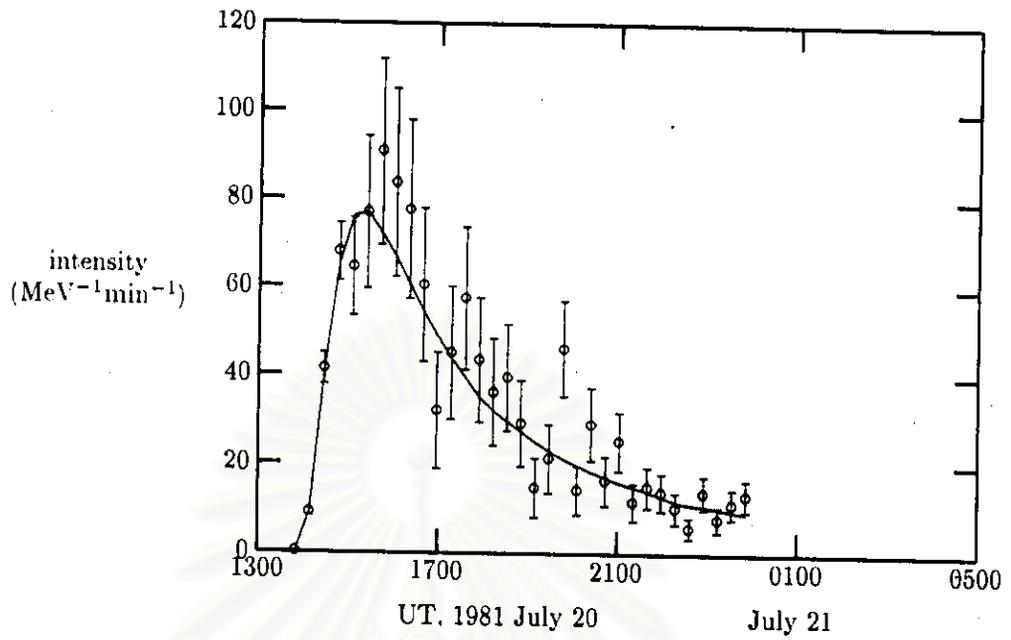


Figure 4.7: Graph of data and simulation of intensity $\lambda=0.12$ AU for energy 4,5 Flare July 20,81.

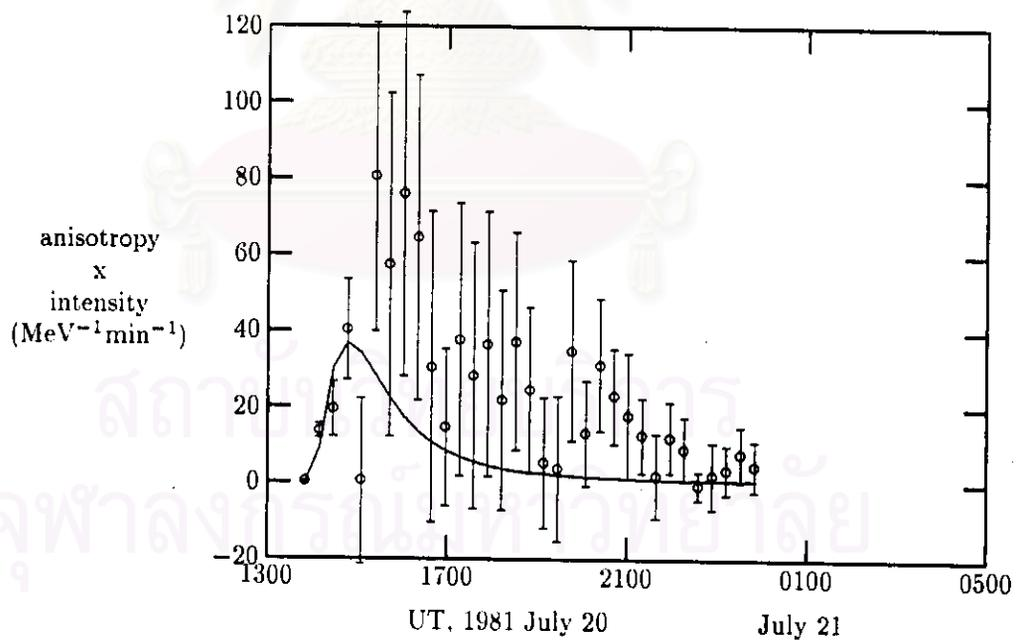


Figure 4.8: Graph of data and simulation of anisotropy $\lambda=0.12$ AU for energy 4,5 Flare July 20,81. The anisotropy is poorly fit because of rapid magnetic field fluctuations.

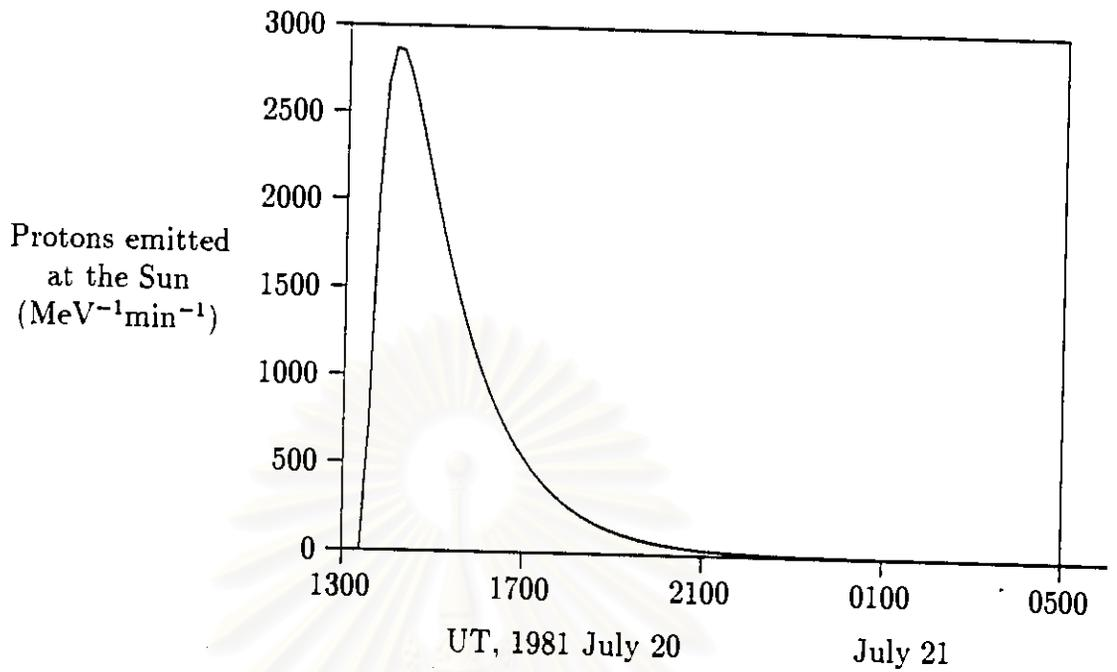


Figure 4.9: Profile of injection for the gradual flare of 1981 July 20 in E1 and $\lambda=0.08$ AU

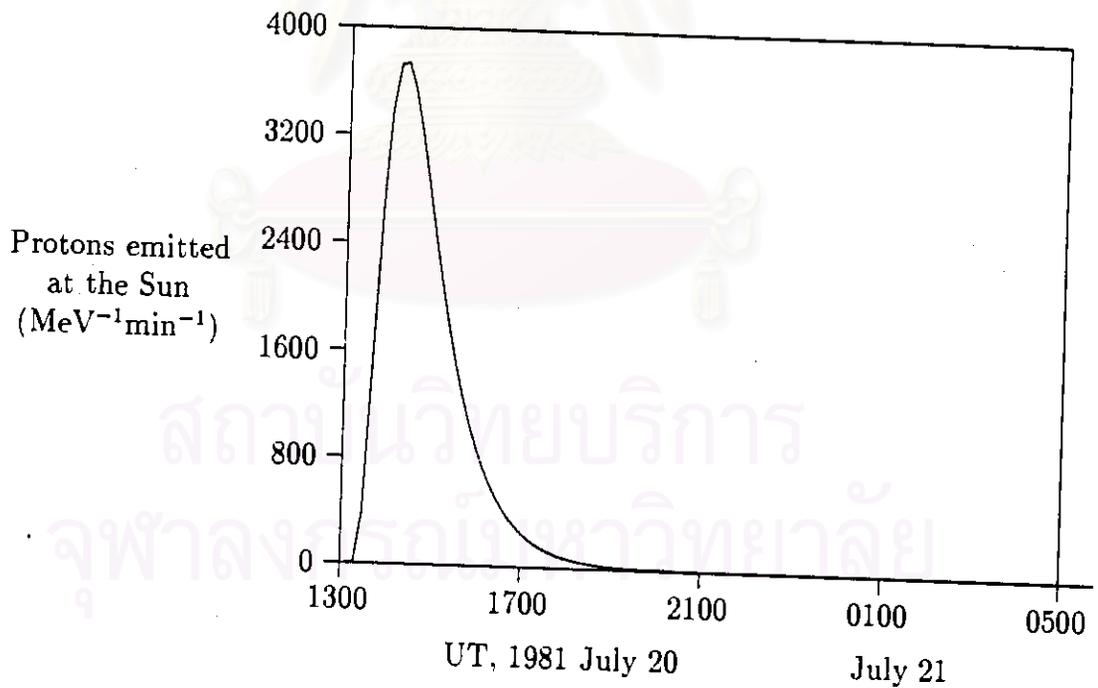


Figure 4.10: Profile of injection for the gradual flare of 1981 July 20 in E2 and $\lambda=0.10$ AU

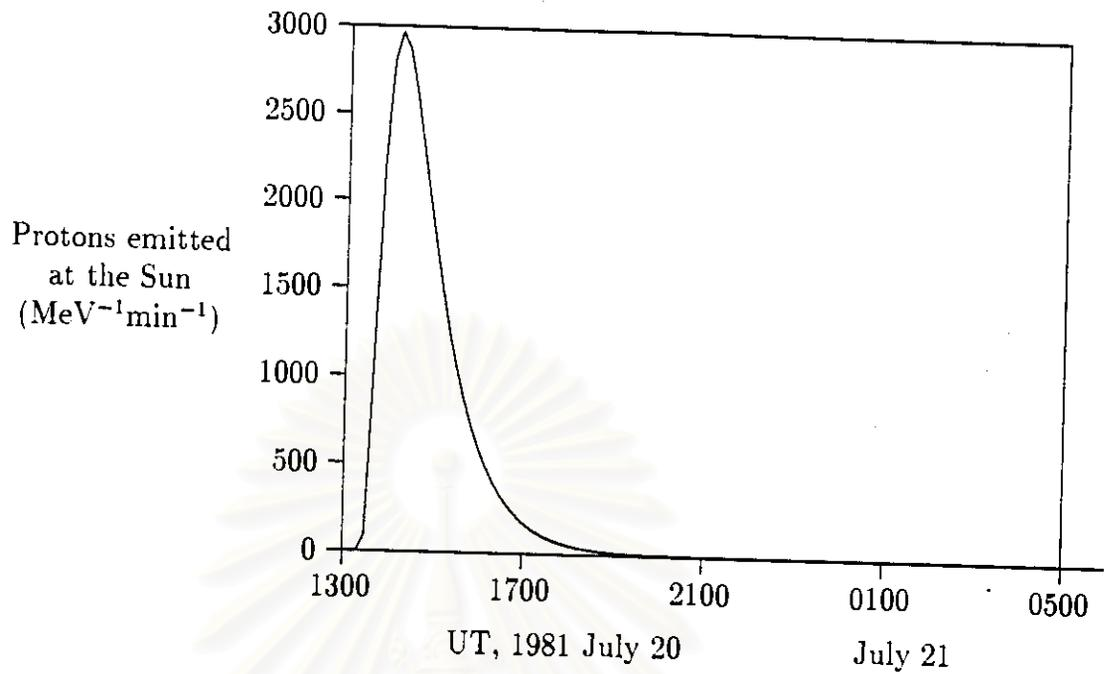


Figure 4.11: Profile of injection for the gradual flare of 1981 July 20 in E3 and $\lambda=0.12$ AU

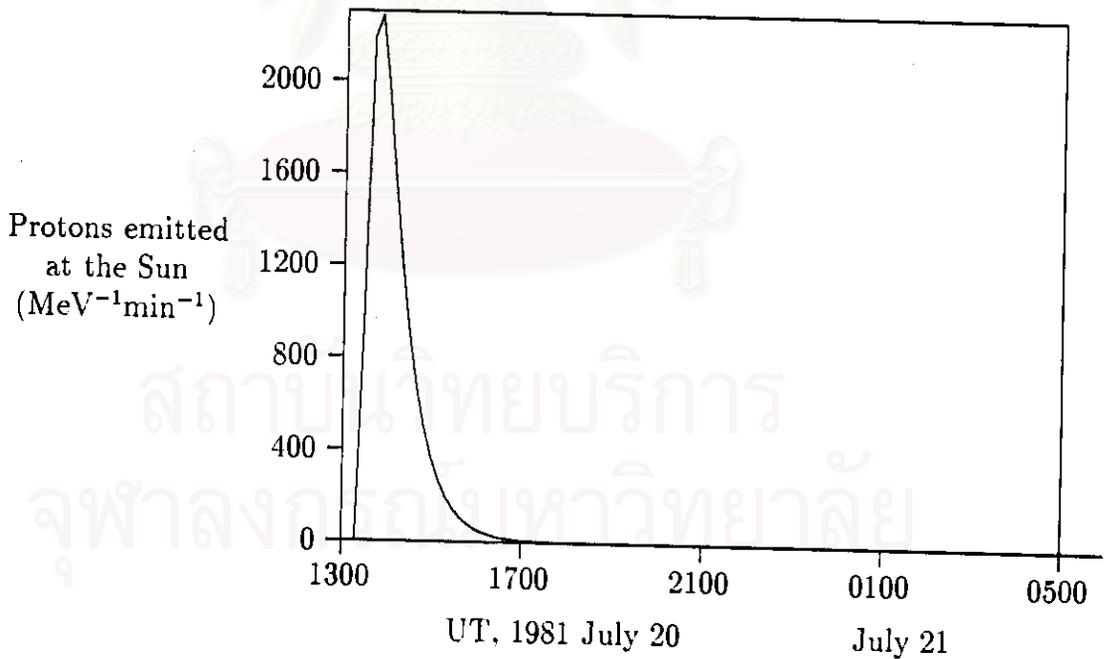


Figure 4.12: Profile of injection for the gradual flare of 1981 July 20 in E4 and $\lambda=0.12$ AU

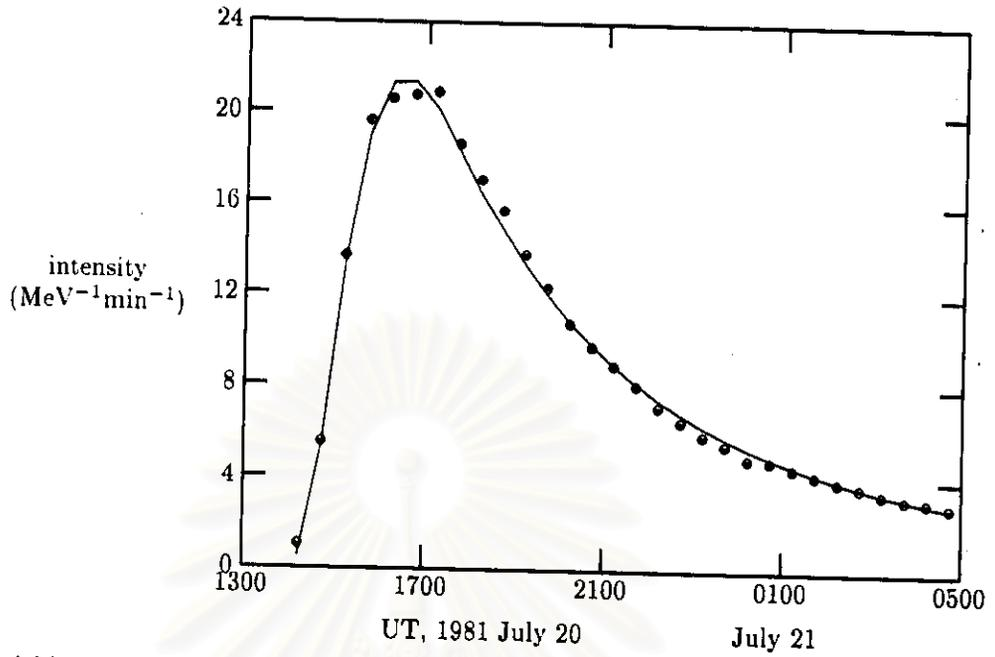


Figure 4.13: Graph of data and simulation of intensity $\lambda=0.10$ AU for the Flare July 20, 1981.

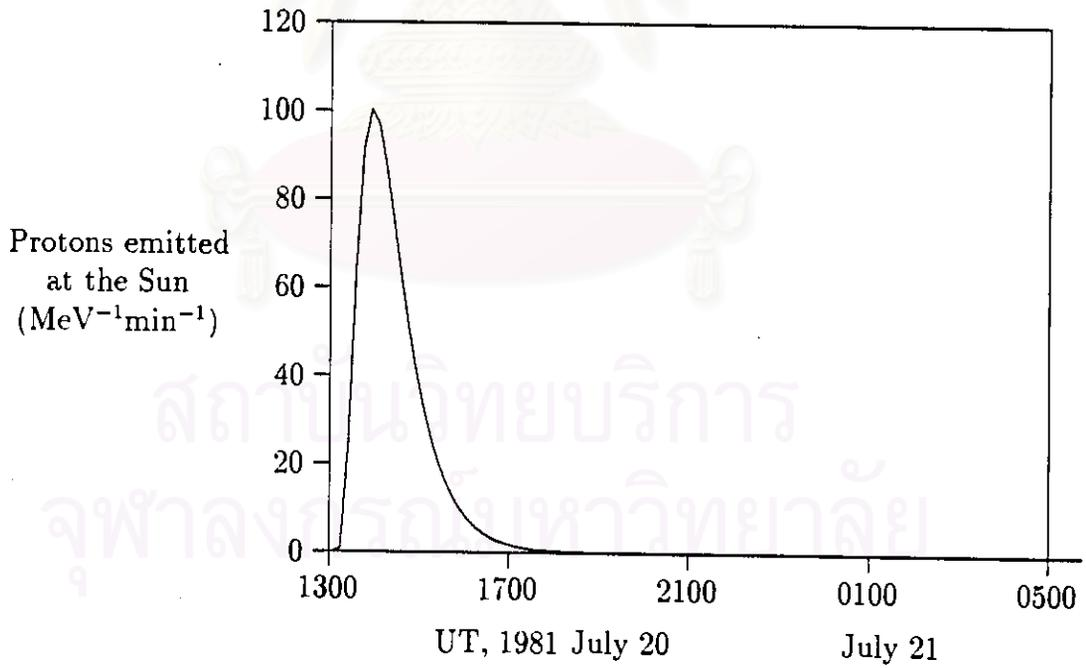


Figure 4.14: Profile of injection for the gradual flare of 1981 July 20 without energy separation and $\lambda=0.10$ AU

λ	Chi-square
0.15	5.706081
0.20	3.702726
0.25	4.076485
0.35	6.145002
0.45	49.199506

Table 4.3: Chi-square values for the impulsive flare of 1982 January 2 in intensity and anisotropy \times intensity vs time.

FWHM	piecewise linear	conjugate direction
E1	195.26	193.57
E2	126.16	95.02
E3	67.50	44.29
E4	35.00	28.23

Table 4.4: Comparison of the two methods by using FWHM for the flare of 1981 January 2.

square 3.703. Graph of this result in intensity is shown in the figure 4.15, figure 4.16 for anisotropy \times intensity and graph of injection profile is shown in the figure 4.17.

Comparison between Piecewise Linear and Conjugate Direction Optimization Method

The comparison of the two methods, piecewise linear and conjugate direction optimization, in full width half max (FWHM) is in the table 4.4 by using the best λ (0.10 AU) for the gradual flare of 1981 July 20, and show in the figure 4.18 that the graphs of these two method have the close results.

The Flare of 1978 September 23 (ULEWAT)

Fitting result in each energy of this flare which the use the ULEWAT data is in the table 4.5. The energies vary from E1 to E4 and λ vary from 0.05

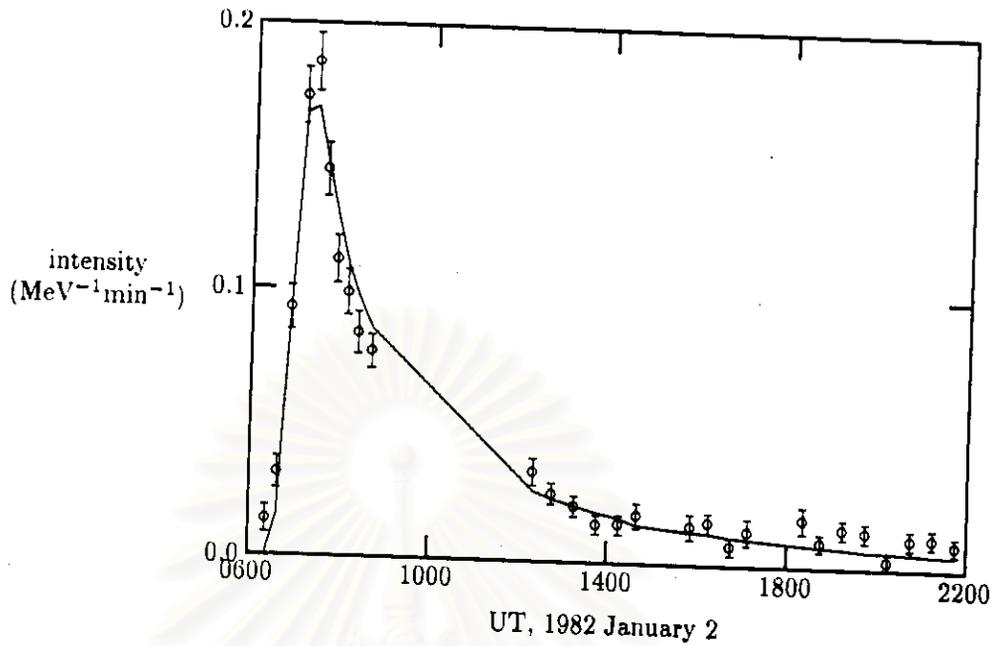


Figure 4.15: Graph of data and simulation of intensity $\lambda=0.20$ AU for the Flare January 2, 1982.

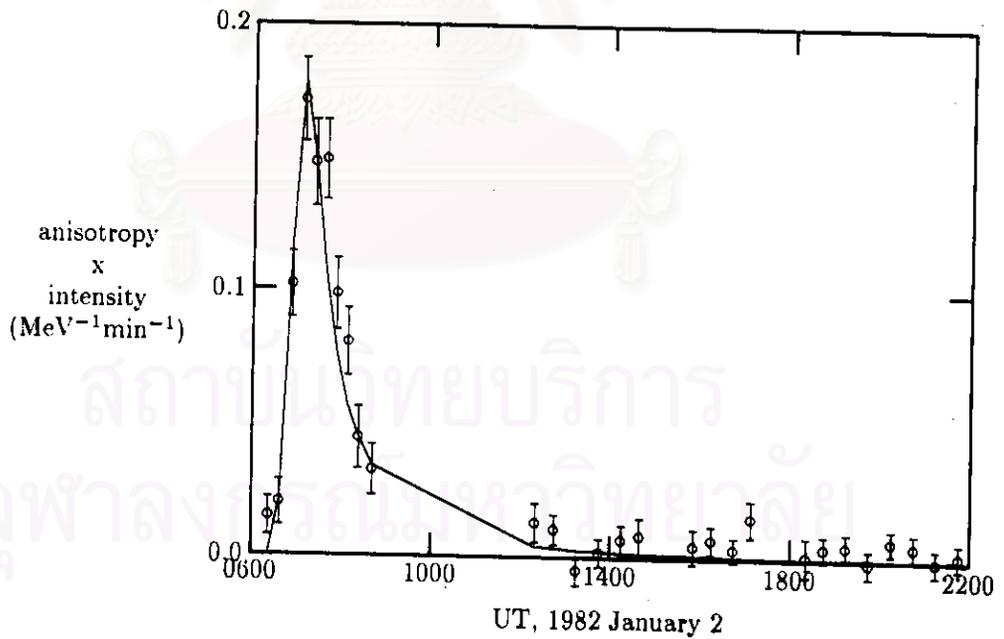


Figure 4.16: Graph of data and simulation of anisotropy $\lambda=0.20$ AU for the Flare January 2, 1982.

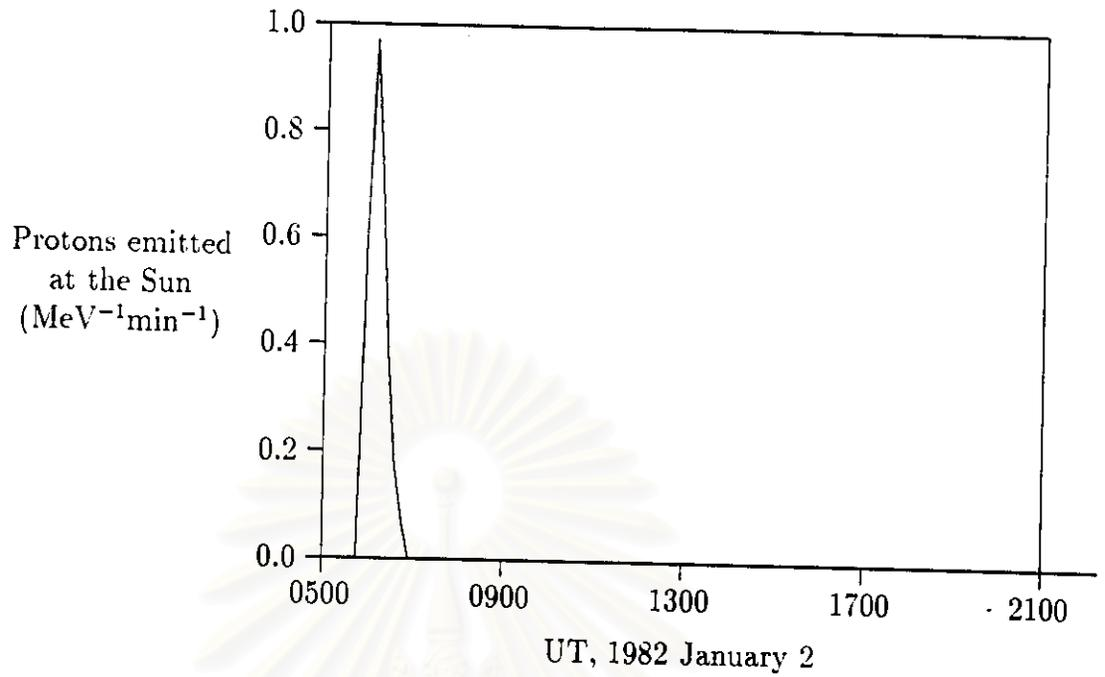


Figure 4.17: Profile of injection for the impulsive flare of 1981 July 20 with $\lambda=0.10$ AU

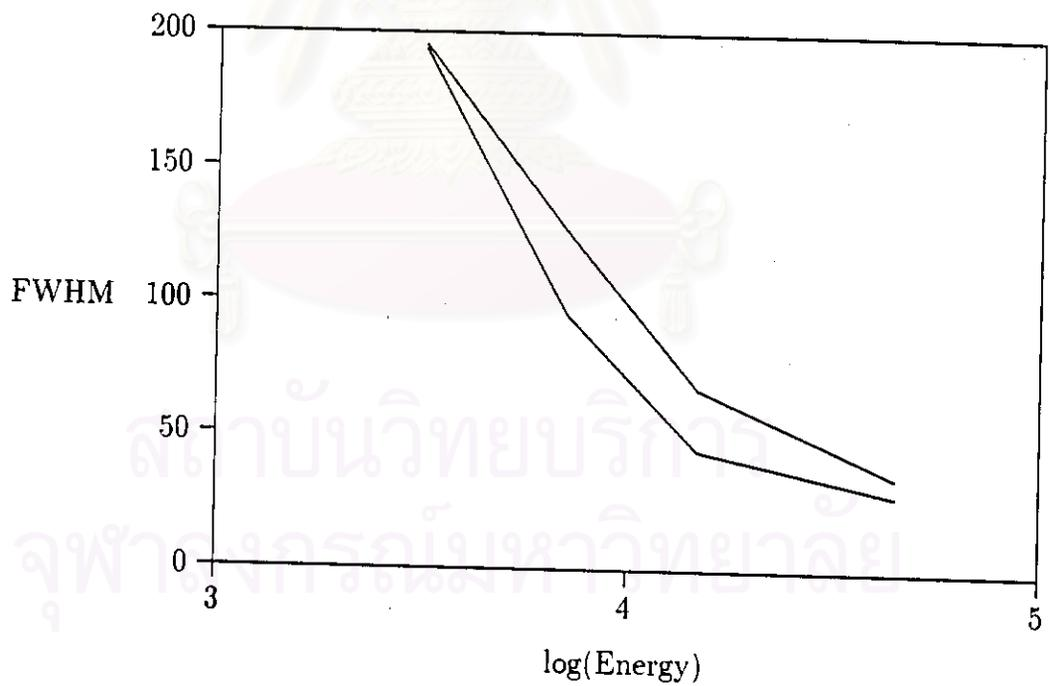


Figure 4.18: Graph of comparison FWHM between piecewise linear method and conjugate direction optimization method.

λ	E1	E2	E3	E4
0.05	2453.100774	1356.991352	112.080997	105.006947
0.08	2688.812743	1134.376978	83.703922	80.861723
0.10	2724.685297	1141.795392	83.148551	83.123792
0.12	2956.657470	1146.658401	85.117429	82.108034
0.15	3682.221547	1138.918067	84.452309	83.892639
0.20	3657.134867	1143.931201	84.614108	87.687781
0.30	4799.865466	1201.092390	93.394527	103.268588

Table 4.5: Chi-square values for the flare of 1978 September 23 (ULEWAT) in each energy.

AU to 0.30 AU. The best λ for E1 is 0.05 AU or lower. For E2,E3 and E4 the best λ is 0.08, 0.10, and 0.12 respectively, graphs of the fitting is shown in the figure 4.19, 4.21, 4.23, and 4.25 respectively and graphs in the figure 4.20, 4.22, 4.24, and 4.26 are shown the injection profile of E1 to E4 respectively.

The Flare of 1978 September 23 (HELIOS I)

Fitting result in each energy of this flare which the use the HELIOS I data is in the table 4.6. The energies vary from E1 to E4 and λ vary from 0.05 AU to 0.25 AU. The best λ for E1 is 0.25 AU. For E2,E3 and E4 the best λ are all 0.25 too, graphs of the fitting is shown in the figure 4.27, 4.29, 4.31, and 4.33 respectively and graphs in the figure 4.28, 4.30, 4.32, and 4.34 are shown the injection profile of E1 to E4 respectively.

The Flare of 1978 September 23 (HELIOS II)

Fitting result in each energy of this flare which the use the HELIOS II data is in the table 4.7. The energies vary from E1 to E4 and λ vary from 0.05 AU to 0.25 AU. The best λ for E1 is 0.08 AU. For E2,E3 and E4 the best λ is 0.10, 0.12, and 0.12 respectively, graphs of the fitting is shown in the figure 4.35,

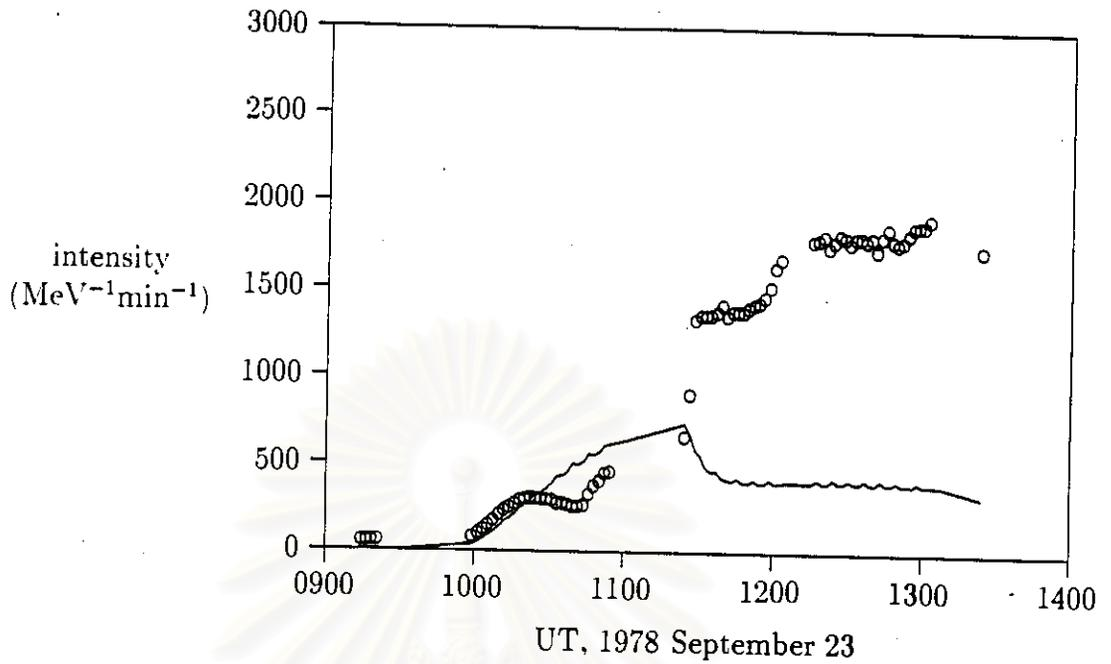


Figure 4.19: Graph of data and simulation of intensity $\lambda=0.05$ AU for energy 1 Flare September 23, 78 (ULEWAT).

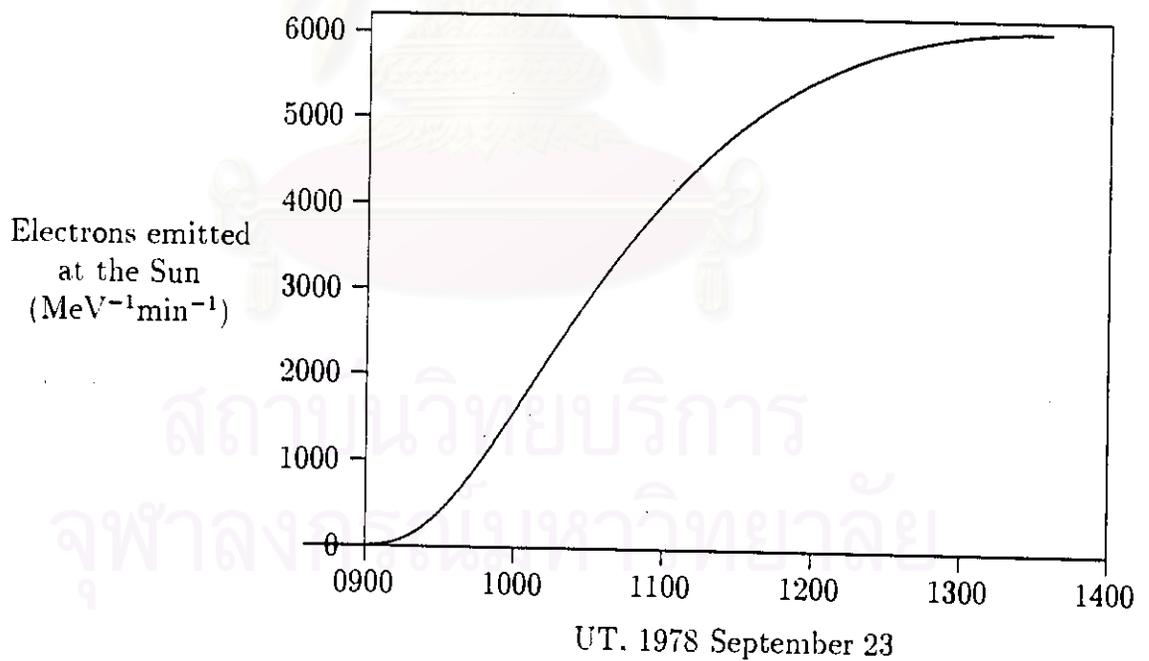


Figure 4.20: Profile of injection for the flare of 1978 September 23 in E1 and $\lambda=0.05$ AU (ULEWAT)

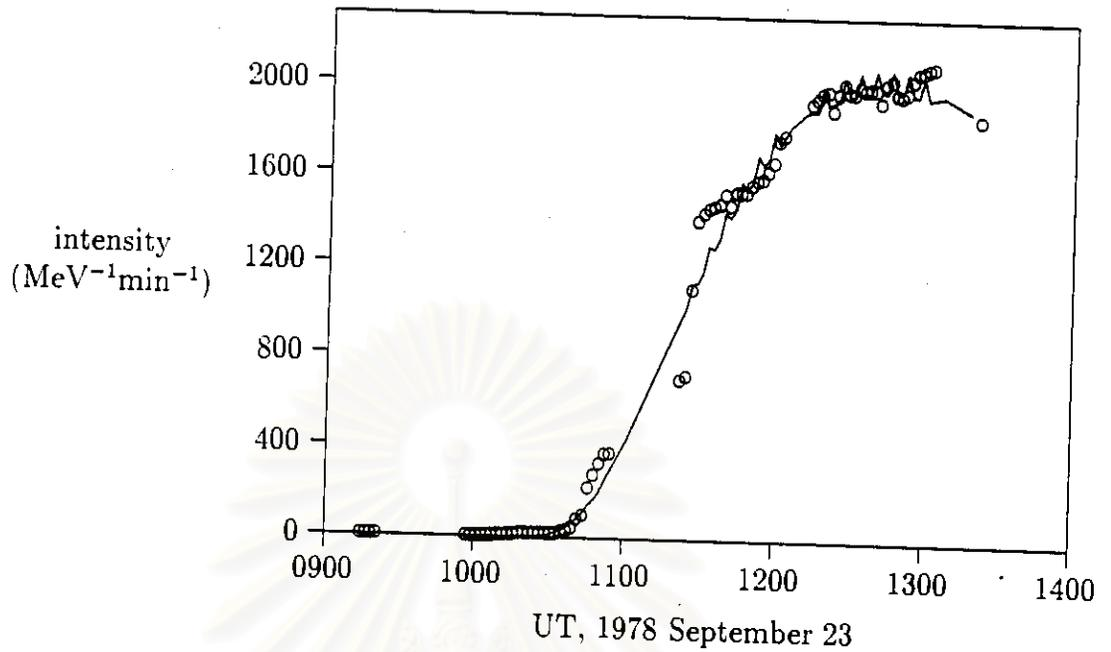


Figure 4.21: Graph of data and simulation of intensity $\lambda=0.08$ AU for energy 2 Flare September 23,78 (ULEWAT).

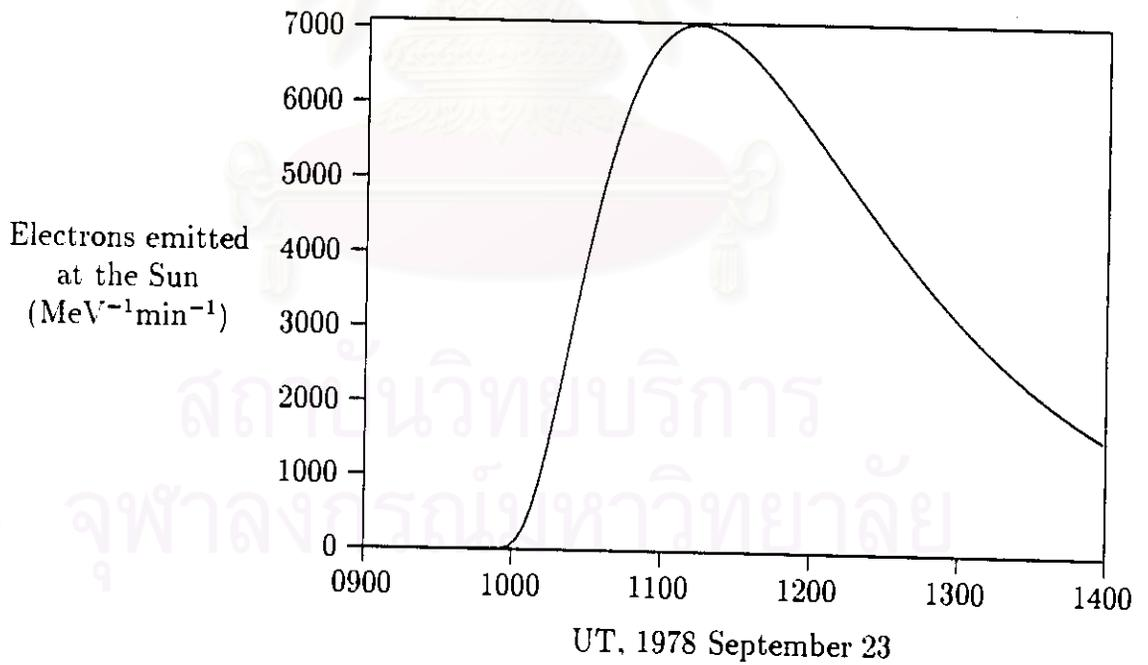


Figure 4.22: Profile of injection for the flare of 1978 September 23 in E2 and $\lambda=0.08$ AU (ULEWAT).

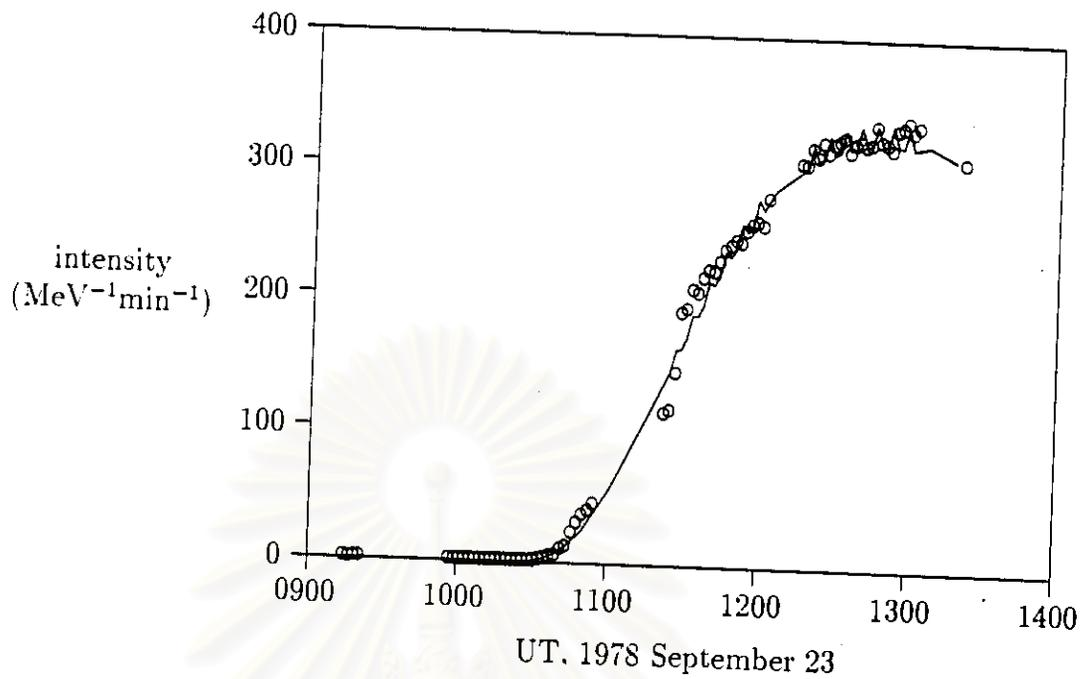


Figure 4.23: Graph of data and simulation of intensity $\lambda=0.10$ AU for energy 3 Flare September 23.78 (ULEWAT).

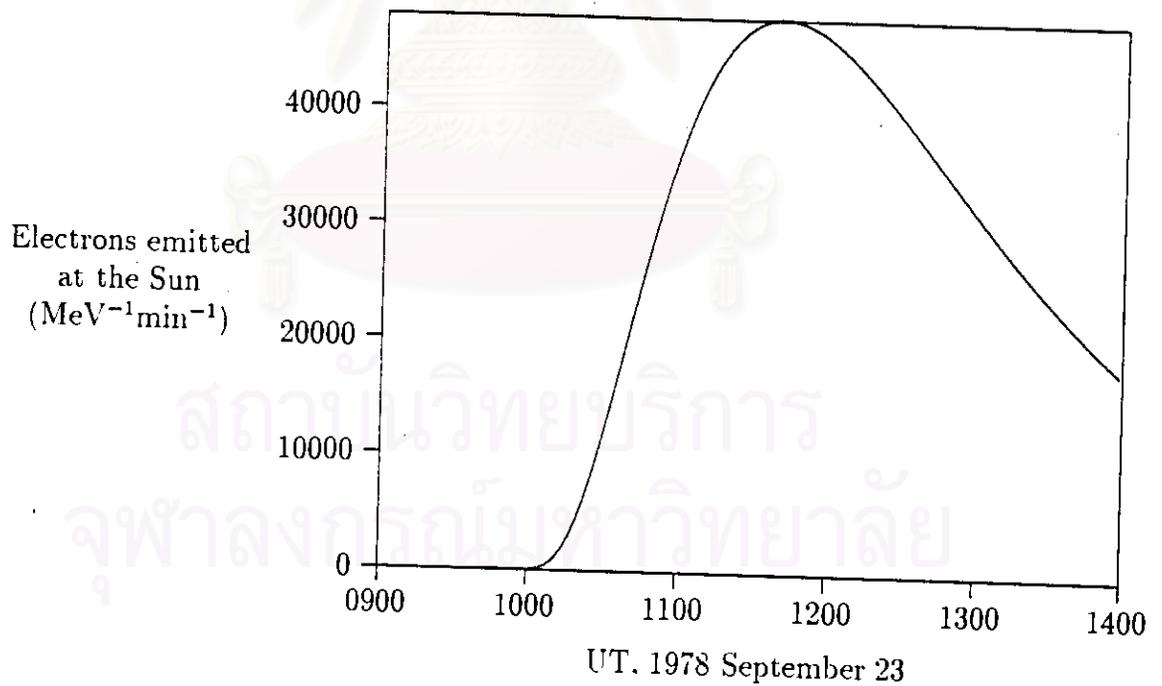


Figure 4.24: Profile of injection for the flare of 1978 September 23 in E3 and $\lambda=0.10$ AU (ULEWAT).

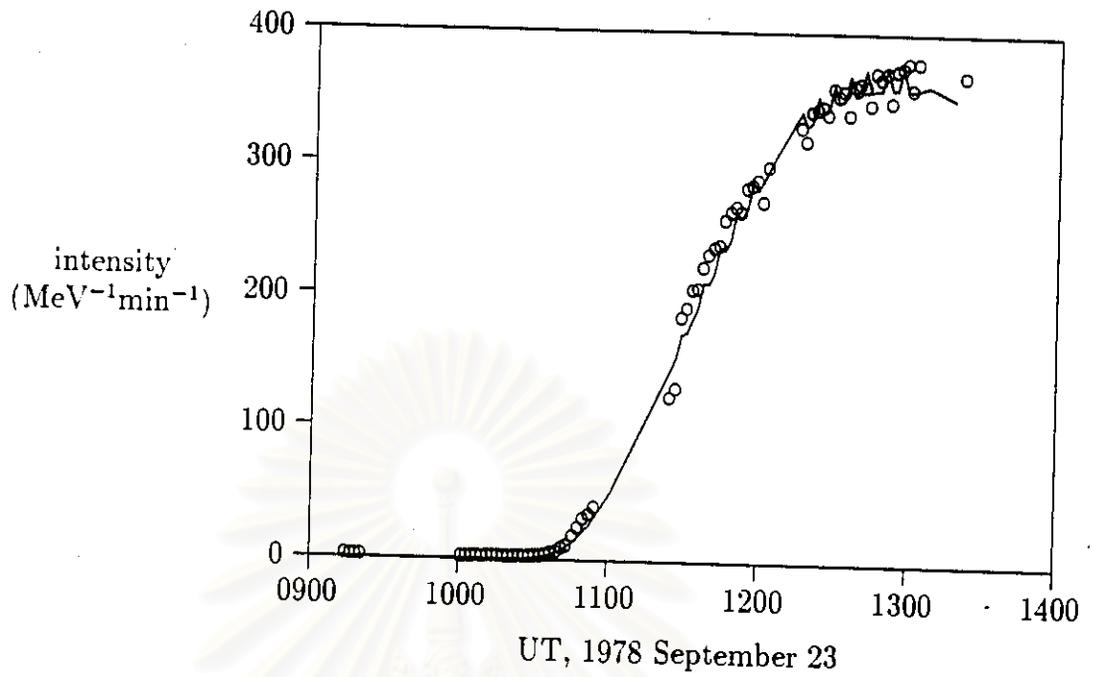


Figure 4.25: Graph of data and simulation of intensity $\lambda=0.12$ AU for energy 4 Flare September 23, 1978 (ULEWAT).

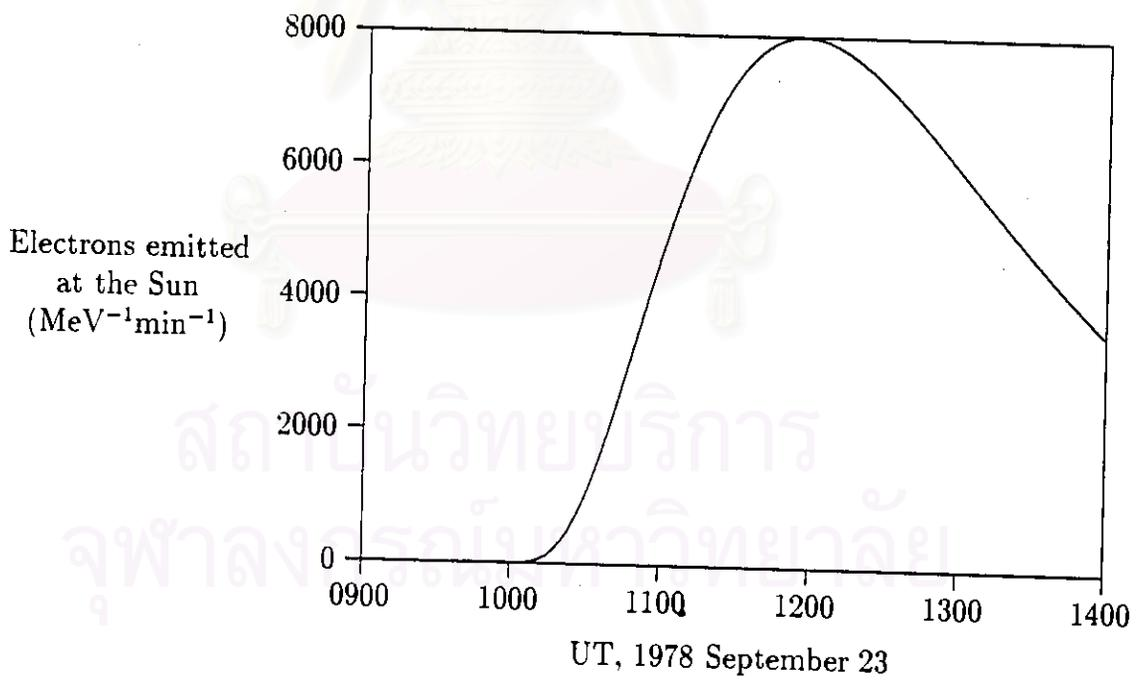


Figure 4.26: Profile of injection for the flare of 1978 September 23 in E4 and $\lambda=0.12$ AU (ULEWAT).

λ	E1	E2	E3	E4
0.05	1804.553500	78.133670	6.035798	1.222136
0.08	3805.347384	95.756492	9.612032	3.257317
0.10	3722.343116	77.476207	8.064338	2.793706
0.12	3564.553319	65.857138	6.758070	2.540594
0.15	3242.951687	53.433709	5.678400	2.178521
0.20	2969.368308	43.362986	4.354324	1.764229
0.25	2810.786184	34.744755	2.890842	1.457079

Table 4.6: Chi-square values for the flare of 1978 September 23 (HELIOS I) in each energy.

λ	E1	E2	E3	E4
0.05	24.793952	3.985746	3.609900	14.334657
0.08	2.427836	1.282712	1.413924	1.472458
0.10	3.747616	1.112697	1.201160	1.108753
0.12	7.971596	1.562227	1.182007	0.994798
0.15	14.320825	2.338675	1.293701	1.006499
0.20	29.741747	3.251940	1.434680	1.004674
0.25	48.725109	9.674932	2.906644	1.684526

Table 4.7: Chi-square values for the flare of 1978 September 23 (HELIOS II) in each energy.

4.37, 4.39, and 4.41 respectively and graphs in the figure 4.36, 4.38, 4.40, and 4.42 are shown the injection profile of E1 to E4 respectively.

สถาบันวิทยบริการ
จุฬาลงกรณ์มหาวิทยาลัย

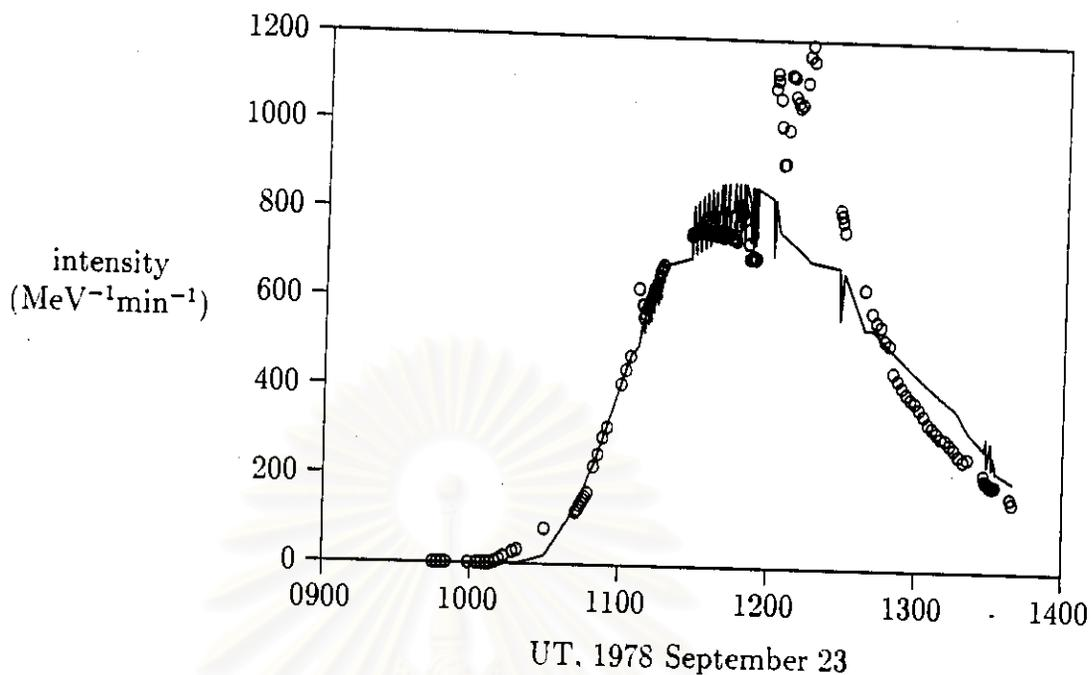


Figure 4.27: Graph of data and simulation of intensity $\lambda=0.25$ AU for energy 1 Flare September 23, 1978 (HELIOS I).

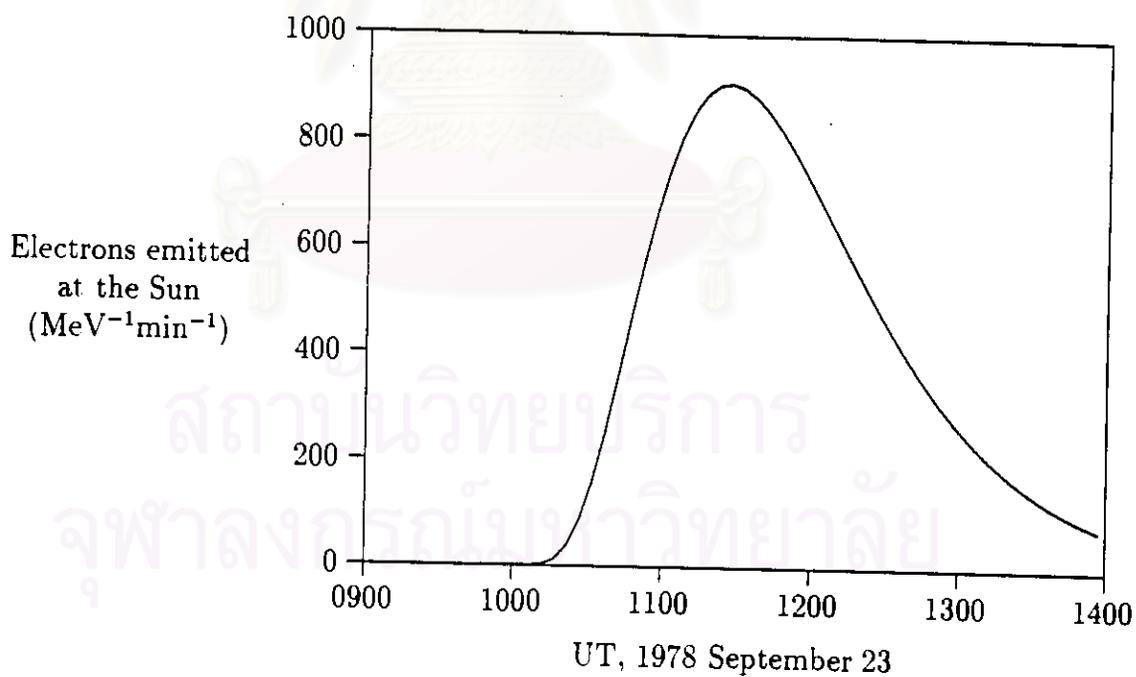


Figure 4.28: Profile of injection for the flare of 1978 September 23 in E1 and $\lambda=0.25$ AU (HELIOS I).

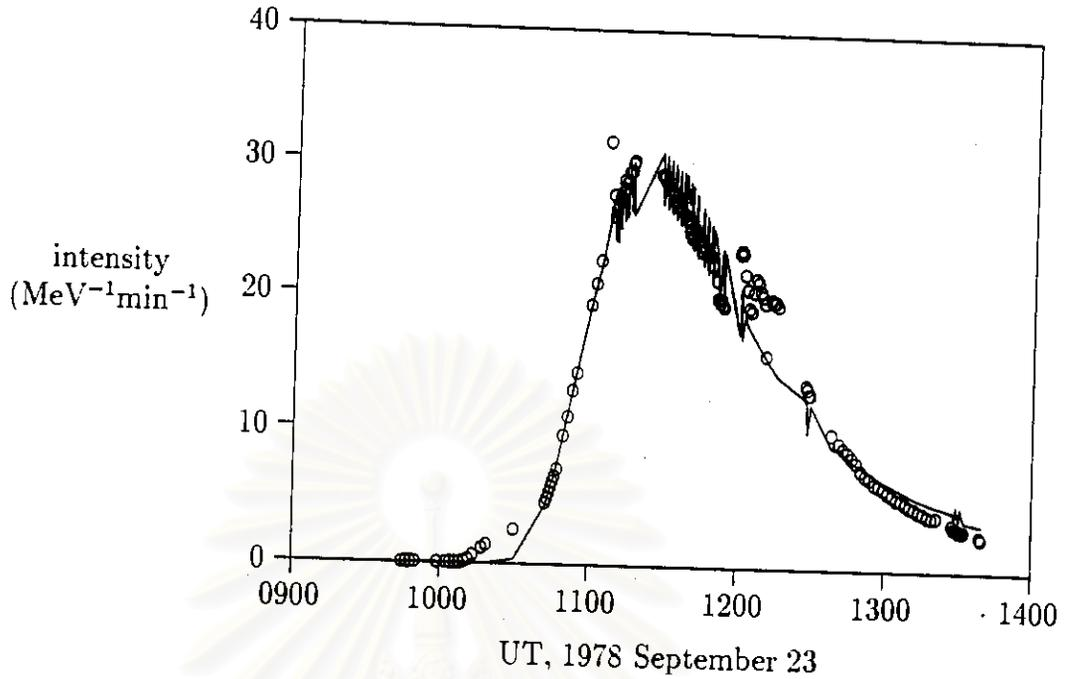


Figure 4.29: Graph of data and simulation of intensity $\lambda=0.25$ AU for energy 2 Flare September 23.78 (HELIOS I).

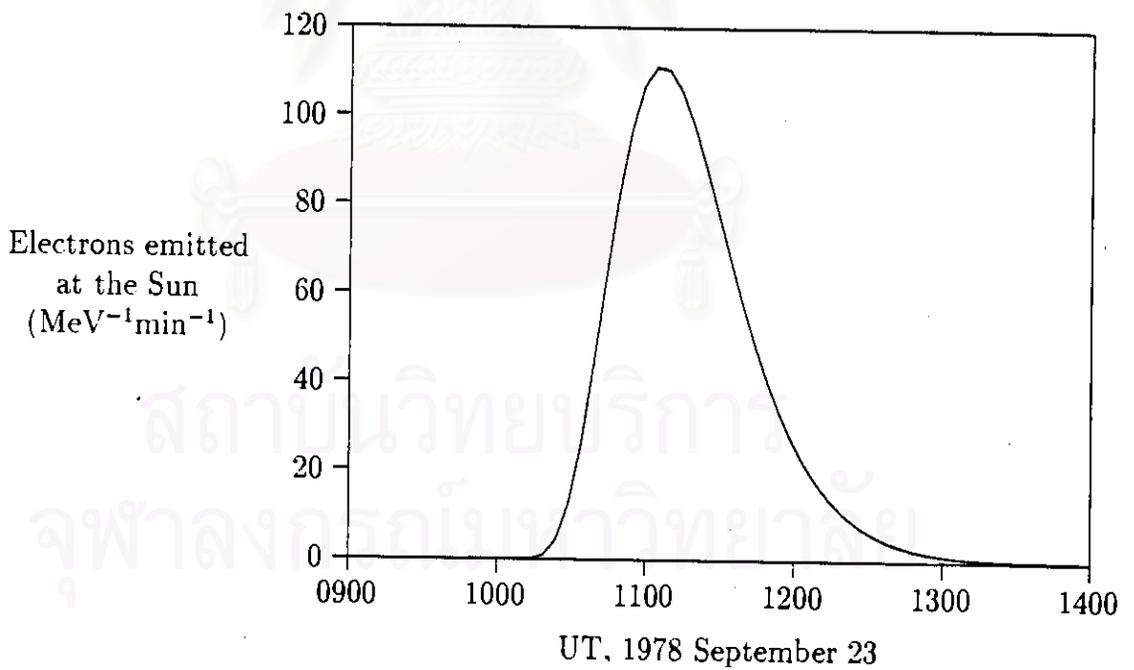


Figure 4.30: Profile of injection for the flare of 1978 September 23 in E2 and $\lambda=0.25$ AU (HELIOS I).

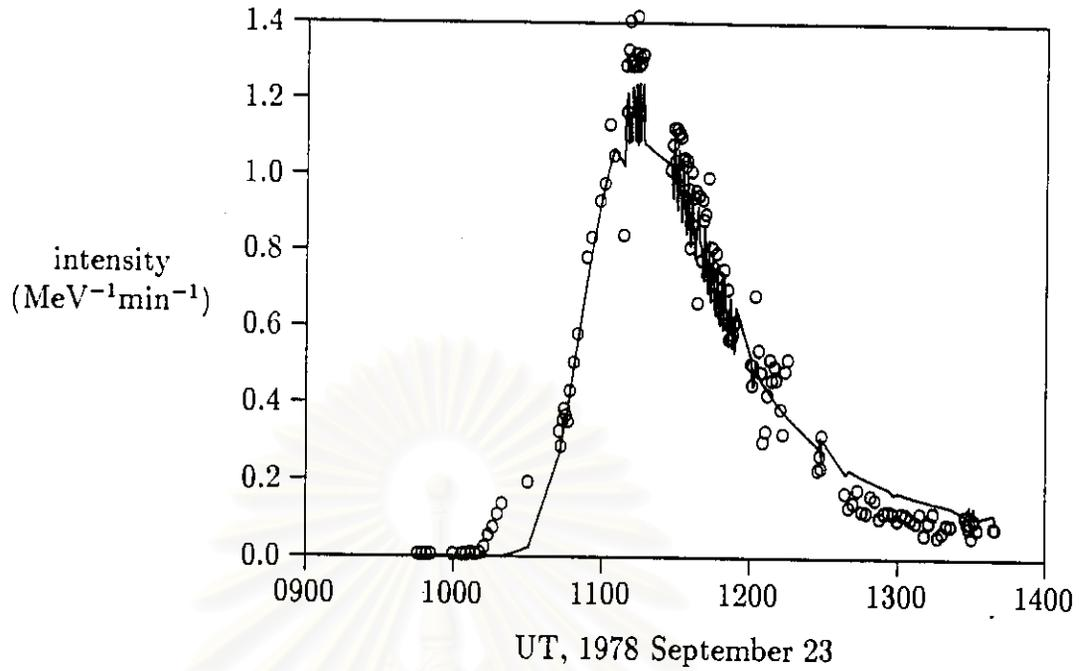


Figure 4.31: Graph of data and simulation of intensity $\lambda=0.25$ AU for energy 3 Flare September 23.78 (HELIOS I).

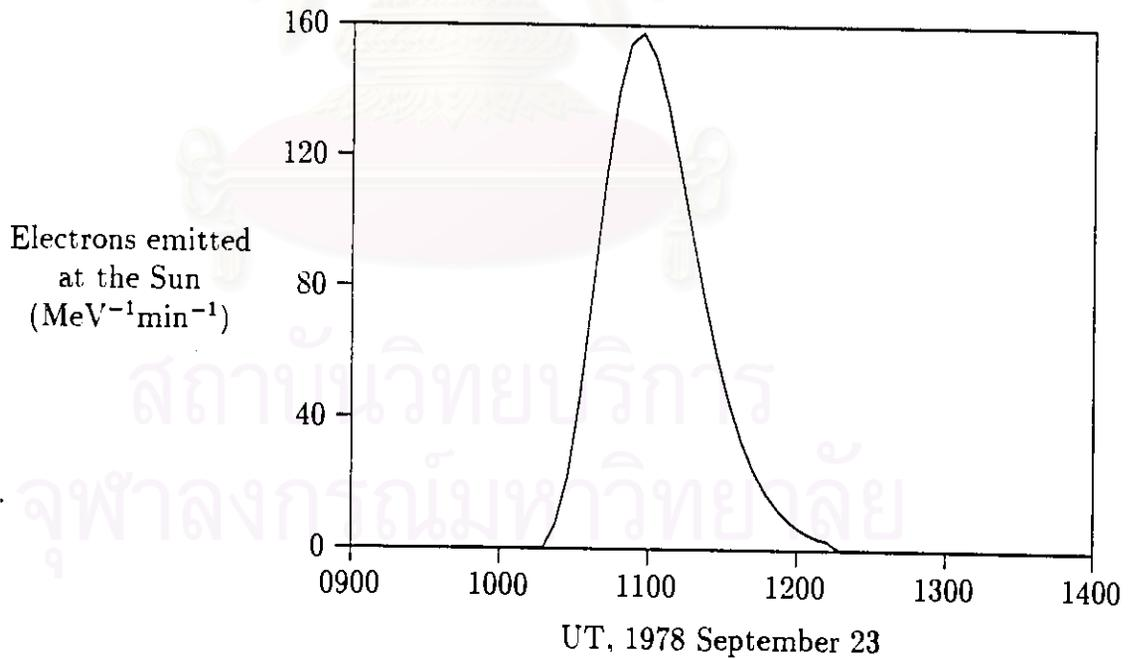


Figure 4.32: Profile of injection for the flare of 1978 September 23 in E3 and $\lambda=0.25$ AU (HELIOS I).

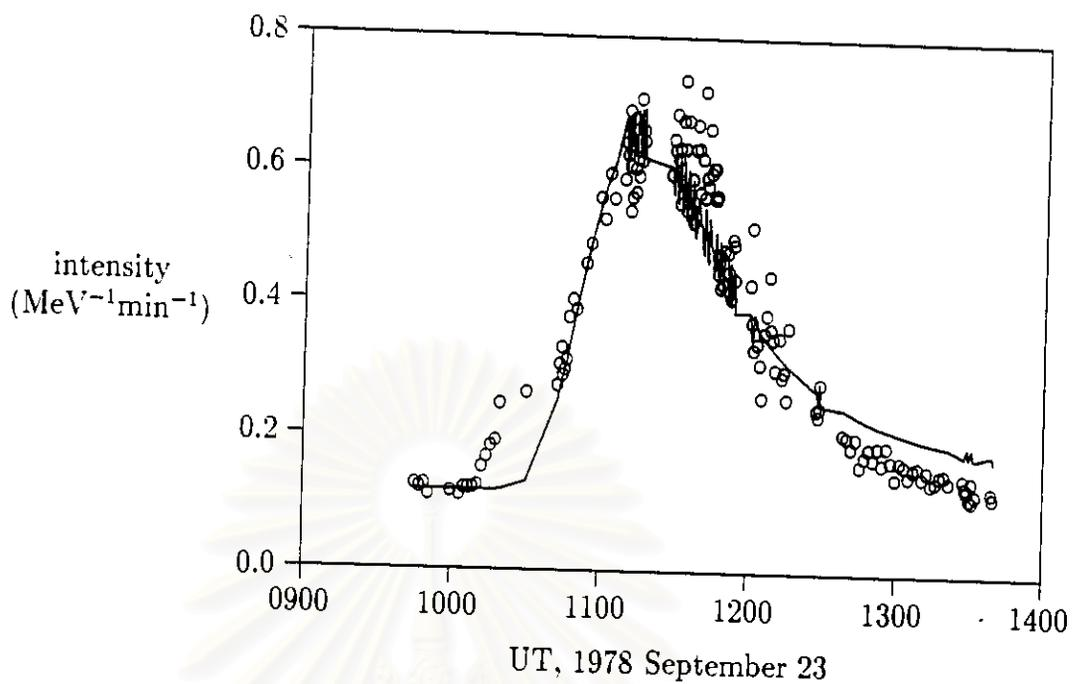


Figure 4.33: Graph of data and simulation of intensity $\lambda=0.25$ AU for energy 4 Flare September 23.78 (HELIOS I).

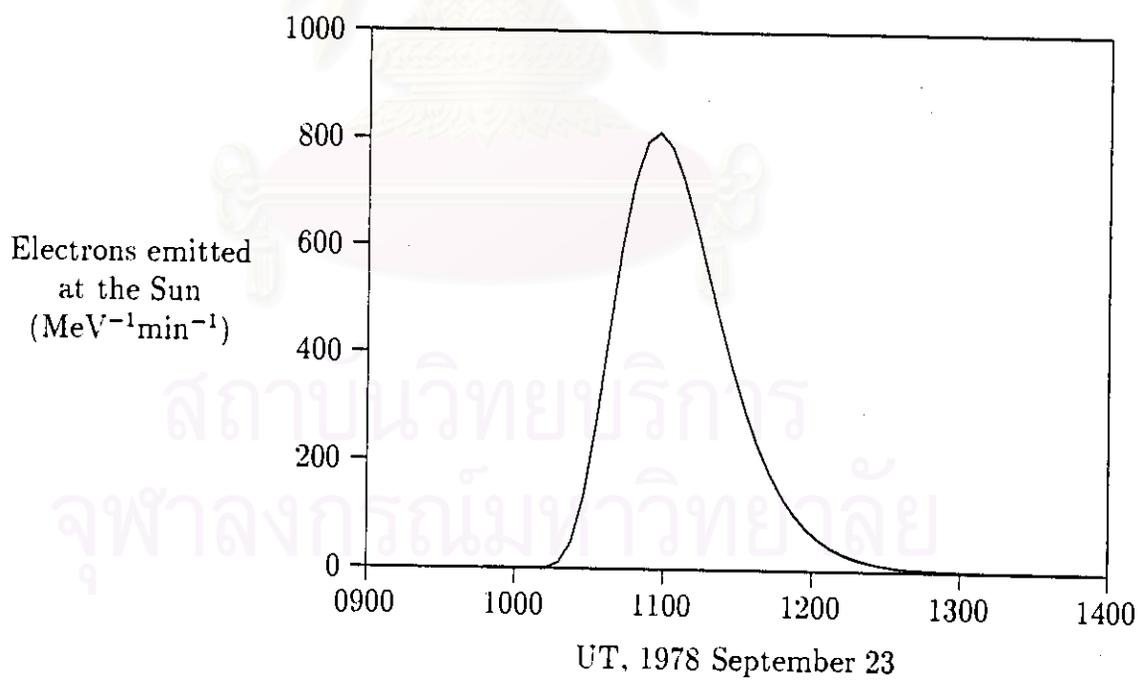


Figure 4.34: Profile of injection for the flare of 1978 September 23 in E4 and $\lambda=0.25$ AU (HELIOS I).

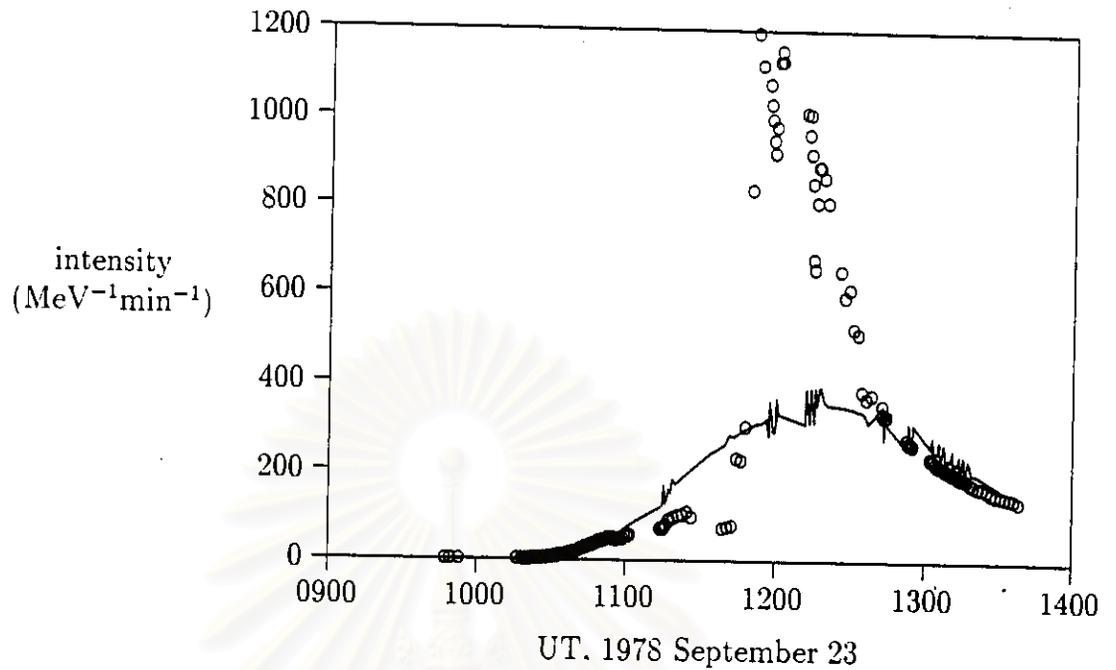


Figure 4.35: Graph of data and simulation of intensity $\lambda=0.08$ AU for energy 1 Flare September 23.78 (HELIOS II).

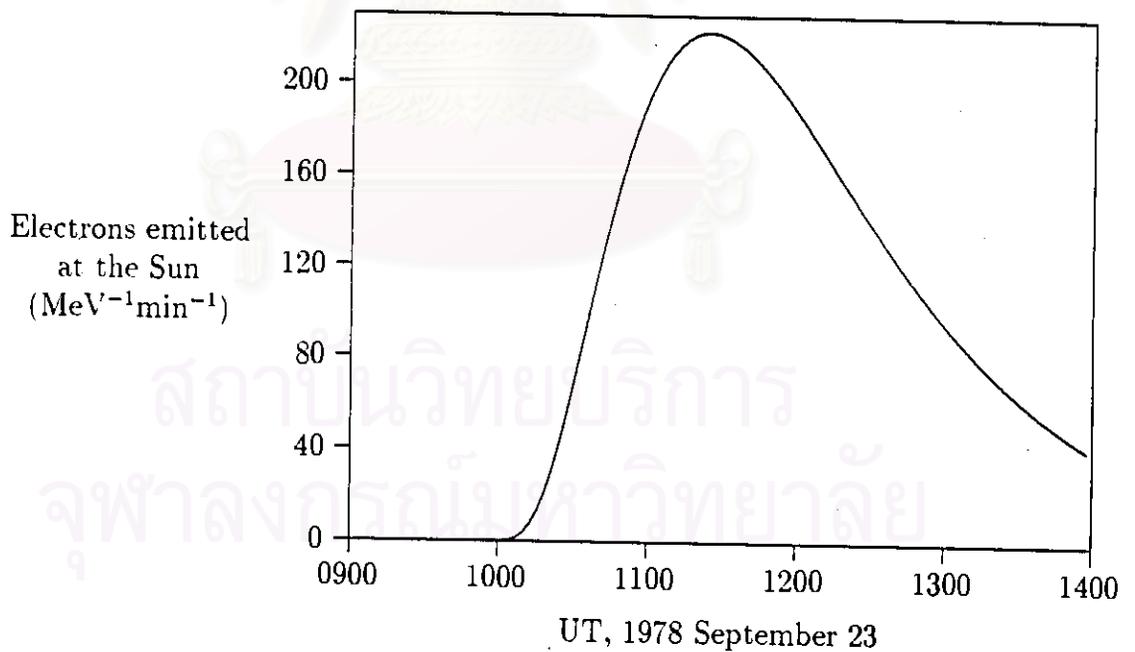


Figure 4.36: Profile of injection for the flare of 1978 September 23 in E1 and $\lambda=0.08$ AU (HELIOS II).

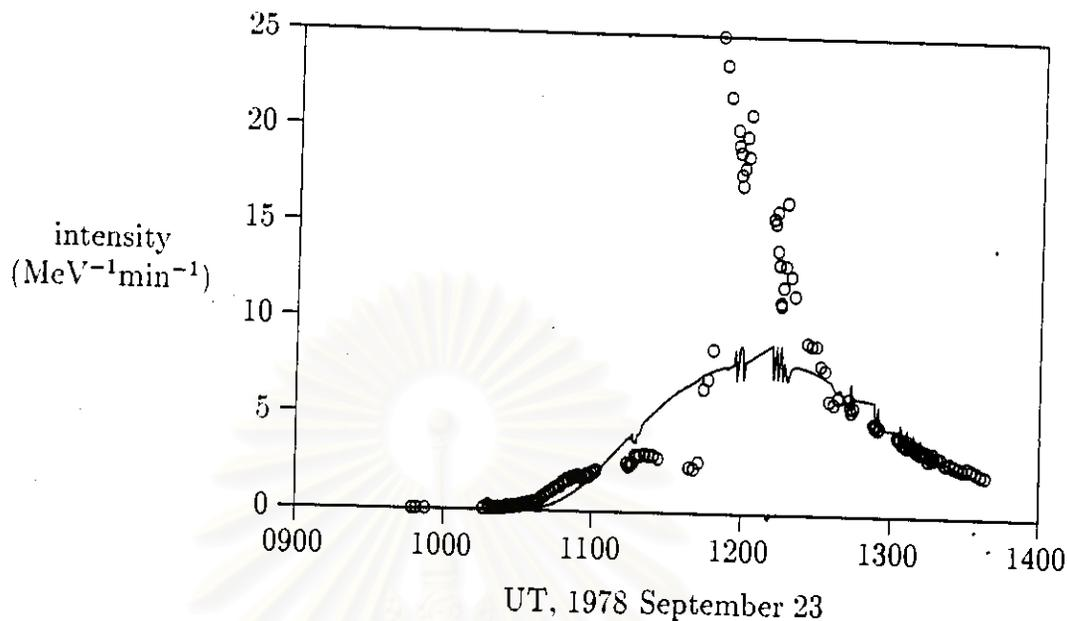


Figure 4.37: Graph of data and simulation of intensity $\lambda=0.10$ AU for energy 2 Flare September 23,78 (HELIOS II).

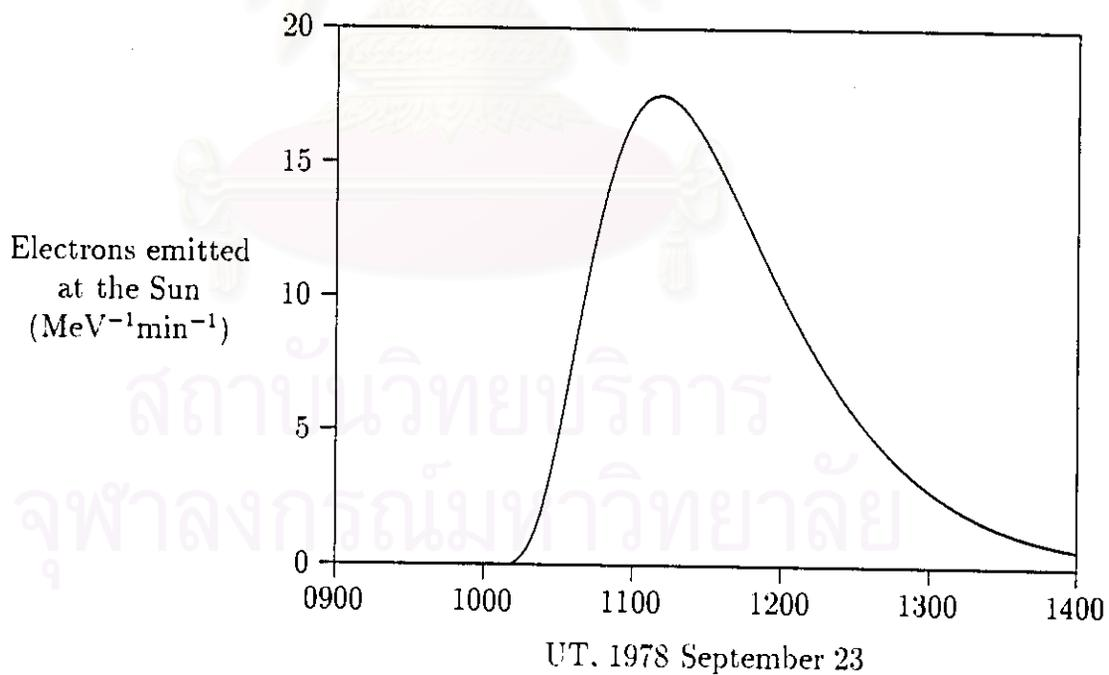


Figure 4.38: Profile of injection for the flare of 1978 September 23 in E2 and $\lambda=0.10$ AU (HELIOS II).

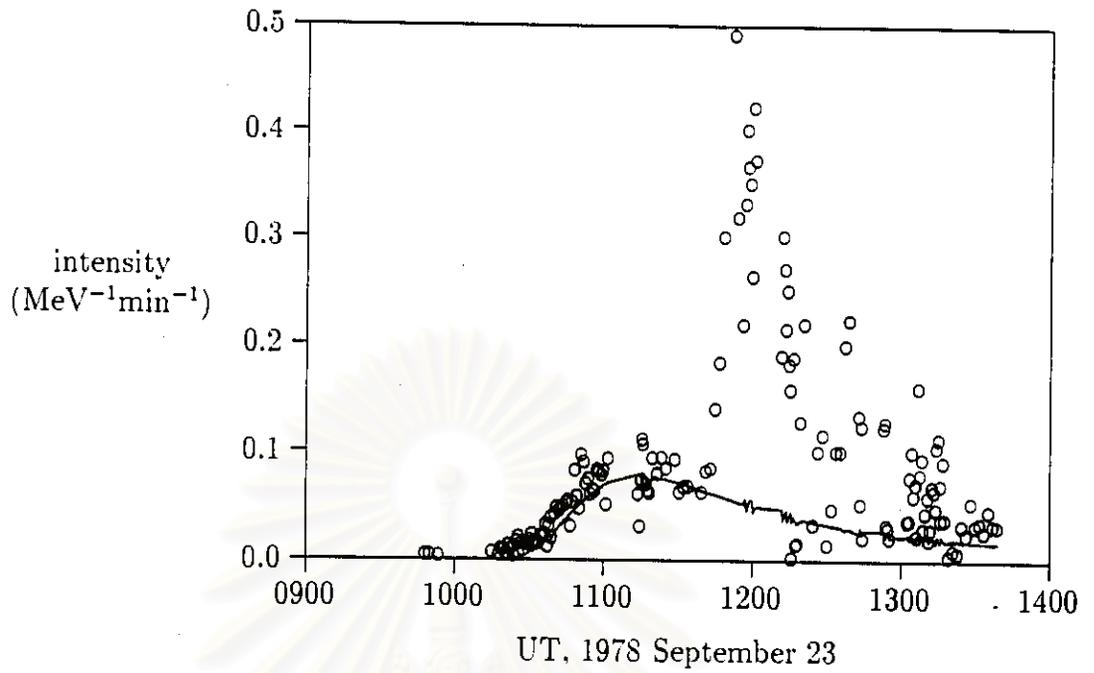


Figure 4.39: Graph of data and simulation of intensity $\lambda=0.12$ AU for energy 3 Flare September 23.78 (HELIOS II).

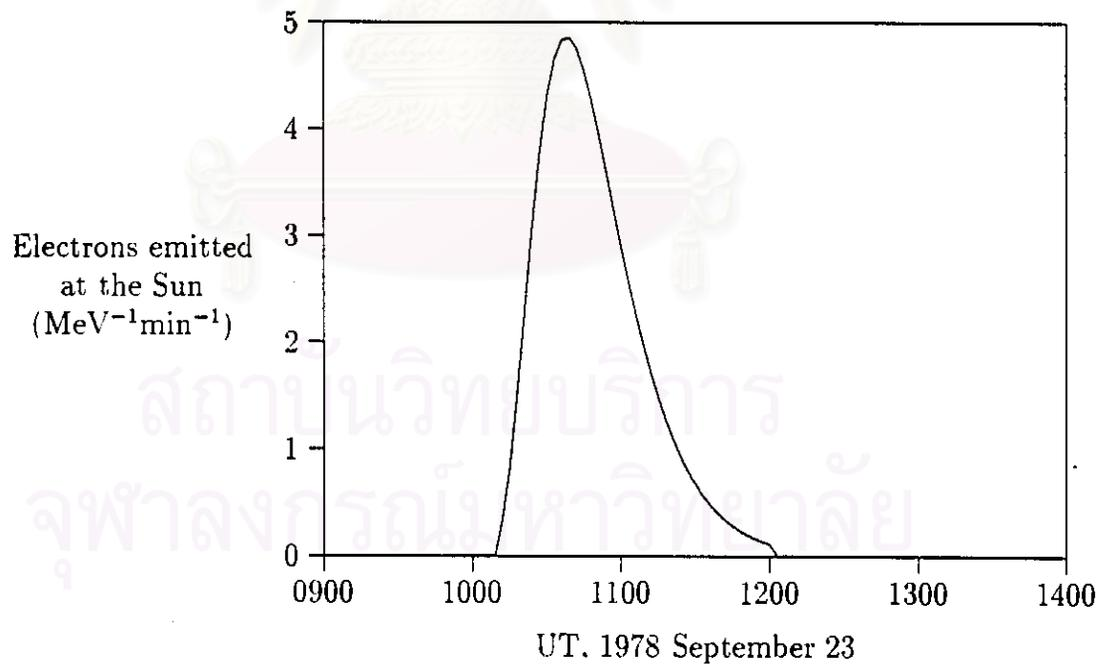


Figure 4.40: Profile of injection for the flare of 1978 September 23 in E3 and $\lambda=0.12$ AU (HELIOS II).

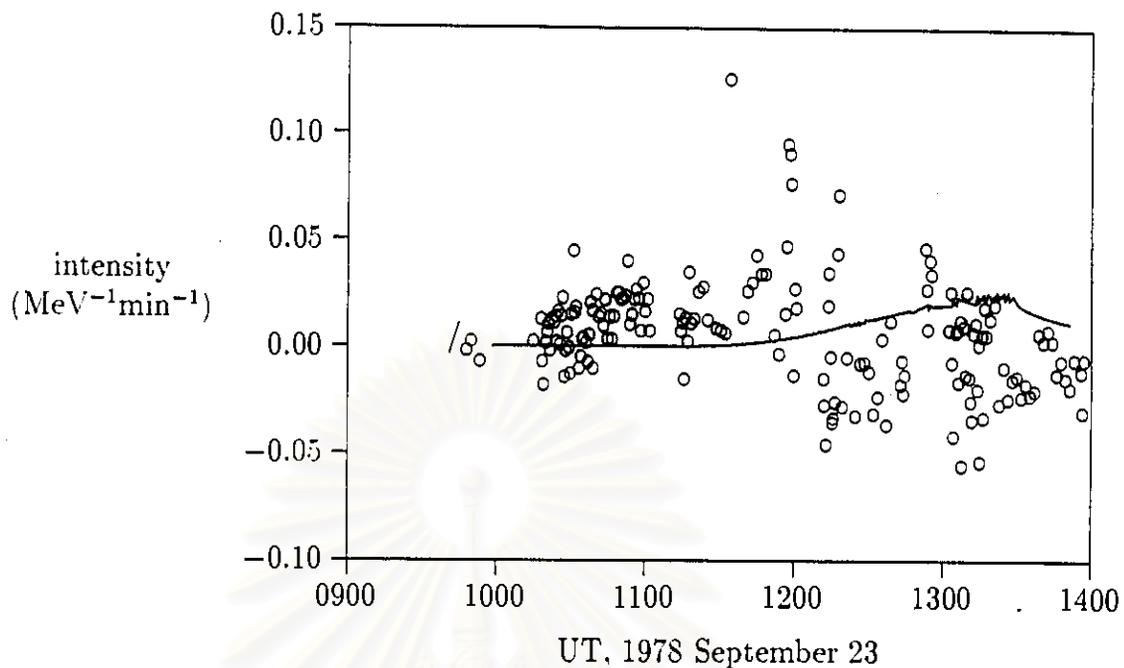


Figure 4.41: Graph of data and simulation of intensity $\lambda=0.12$ AU for energy 4 Flare September 23,78 (HELIOS II).

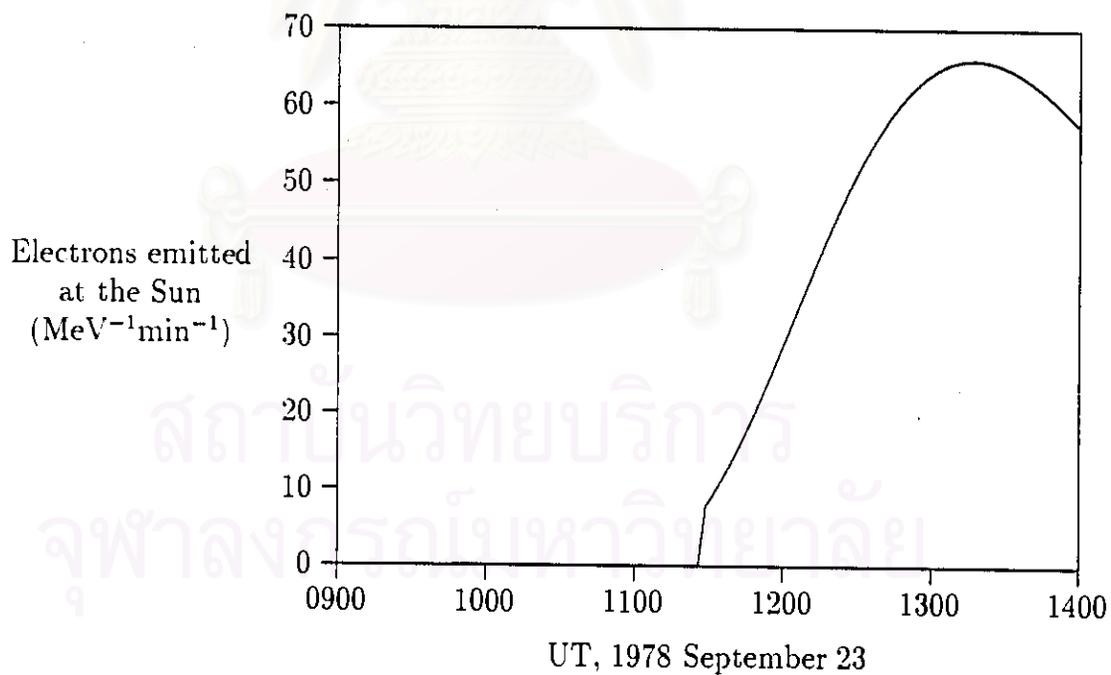


Figure 4.42: Profile of injection for the flare of 1978 September 23 in E4 and $\lambda=0.12$ AU (HELIOS II).